Effect of Platelet Rich Plasma on Regeneration of Submandibular Salivary Gland of Albino Rats.

Wafaa Yahia Ibrahim Elghonamy, Prof. Dr. Olfat Mohammad Gaballah and Dr. Souzan Anwar El Amy

Oral Biology Department, Faculty of Dentistry, Tanta University, Egypt.

Abstract: Background: Extra-oral SMD ligation causes parasympathetic nerve damage which is accompanied by a severe SMG atrophy that may be irreversible. Cell-based therapies using PRP receive great attention in regeneration of various tissues. **The aim of the study** was to assess the effect of SMD ligation on rat SMG with inclusion of the chorda tympani nerve, examine the microscopic structure of SMG after parasympathetic denervation, and to investigate the effect of locally injected PRP on regeneration of SMG after duct deligation in Albino rats. **Methods:** The study sample was consisting of 50 adult male Albino rats. Forty rats were randomly divided into two equal experimental groups; group I was subjected to extra-oral SMD ligation for two weeks and left without any treatment after duct deligation, and group II was subjected to extra-oral SMD ligation for two weeks and treated with PRP at the time of deligation. The remaining ten rats were used for PRP extraction. The left SMGs were used as negative control in both groups. Five rats of each group were scarified at day zero, just after deligation, and before any treatment to evaluate the effect of ligation and then on 3, 7 and 14 days after deligation respectively. The rats were anesthetized, and the specimens of SMG were collected and prepared for LM investigation using H & E and Masson trichrome stains. **Results:** qualitatively, in positive control group, LM results of right SMGs revealed marked degenerative changes persisted on all follow up periods and the severity of these changes was increased gradually from day zero to 14. LM results of the left (unligated) SMGs showed almost normal histological appearances for both groups. Nonetheless, in PRP group clear regeneration of SMG tissues was appeared at follow up periods 7 and 14. **Conclusion**: Our study showed that extra-oral SMD ligation causes severe irreversible atrophic changes of SMG tissues. Moreover, PRP appeared to be histologically effective in the regeneration of SMGs.

[Wafaa Yahia Ibrahim Elghonamy, Olfat Mohammad Gaballah and Souzan Anwar El Amy. **Effect of Platelet Rich Plasma on Regeneration of Submandibular Salivary Gland of Albino Rats.** *N Y Sci J* 2018;11(12):27-40]. ISSN 1554-0200 (print); ISSN 2375-723X (online). http://www.sciencepub.net/newyork. 3. doi:10.7537/marsnys111218.03.

Key words: Submandibular gland (SMG); Submandibular duct (SMD) ligation; parasympathetic denervation; deligation; Platelet rich plasma (PRP).

1. Introduction

The paired Submandibular glands (SMGs) are major salivary glands (SGs) in humans and rodents. The main function of SGs is saliva secretion that is important in lubrication, digestion, immunity, and the overall maintenance of homeostasis within the human body. Additionally, SGs are innervated by postganglionic nerve fibers of the sympathetic and parasympathetic divisions of the autonomic nervous system supply [1,2].

Atrophy of the SGs often due to trauma, sialadenitis, SGs tumors, Sjogren's syndrome, head and neck chemotherapy or radiotherapy. Such atrophy seriously affects salivary secretion leading to xerostomia and consequently oral mucositis [3,4]. Several studies considered ligation of SMD has contributed to understanding the pathology of duct obstruction. Noteworthy, duct ligation causes several atrophic changes vary according to surgical approach, location and period of ligation. Moreover, these changes may be reversible or irreversible [5,6]. Also, previous studies reported that an extra-oral SMD ligation through neck incision cause parasympathetic nerve damage with severe irreversible SMG atrophy [5].

Outstandingly, the goal of regenerative medicine is to restore SGs structure and function in patients who suffer from irreversible loss of SGs function due to atrophy [7]. Platelet rich plasma (PRP) is considered important therapeutic tool in regenerative therapy as it is biological source for growth factors and cytokines essential for regeneration of damaged tissues [8,9]. It gives promising results in tissues other than SGs on regenerative therapy studies through different growth factors and bioactive substances that entrapped within the platelets and orchestrated the tissue regeneration [10].

Therefore, the present study was intended to provide a new research stand through exploring the possible therapeutic effect of local injection of PRP on regeneration of denervated SMGs.

Aim of the Study

The aim of the study was to assess the effect of SMD ligation on rat SMG with inclusion of the chorda tympani nerve, examine the microscopic structure of SMG after parasympathetic denervation, and to investigate the effect of locally injected PRP on

regeneration of SMG after duct deligation in Albino rats.

2. Materials and Methods

A total 50 adult male albino rats aged between 8-10 weeks (200-250 grams) were used in this study. PRP were isolated from 10 rats. The remaining 40 rats were subjected to extra oral right SMD ligation then had been deligated after two weeks. Afterward, the animals were randomly divided into one control group and one experimental group each one contained 20 rats.

Group I (positive control group):-

Rats in this group were subjected to SMD ligation for two weeks and were left without any treatment after ligation. Also, they were subjected to intraglandular (IG) injection with 1 ml sterile physiological saline at the time of deligation to control the influence of injection stress in the experimental groups.

Group II (PRP treated group):-

Rats in this group were subjected to SMD ligation for two weeks and treated with IG injection of isolated PRP solution at the time of deligation.

- Left SMGs in each group were used as negative control for each experimental counterpart.

PRP preparation:

PRP was obtained from10 rats through the following sechedule [(11)].

1. 4 ml blood of anaethized rat was drawn by small syringe via cardiac puncture.
2. 2 ml of the fresh blood was placed into a tube containing EDTA for platelet count into whole blood by using automated cell counter.
3. 1.8 ml of the blood was injected into a tube containing 3.8% sodium citrate for PRP separation and it was centrifuged at 800 RPM for 15 min at room temperature.
4. After centrifugation, the blood cells were precipitated at the bottom and yellow tinted plasma was collected in the upper half**.**
5. The plasma was drawn carefully using 10 cm syringe and inserted in 3.8% sodium citrate tube to be counted.

- The average platelet count present in the whole blood was $850x10^3/\mu l$ and in plasma was $824x\ 10^3/\ \mu l$ in approximately 90 µl.
- Rats in this group were received PRP (0.5 mL/kg body weight) [platelet count, $824 \times 10^3/\square L$] (12) that was injected IG at the center of right SMG at the time of deligation.

Then, SMG tissues were evaluated histologically at days zero, 3, 7, and 14 from deligation respectively. The tissue investigations were done under LM using H & E and Masson trichrome stains to evaluate regeneration of parenchymal elements and collagen fibers respectively.

3. Results

(1) Positive control group (right side):-

A) Day zero:

1. Haematoxylin and Eosin:

Light microscopic examination of SMG of the tissue sections of right SMG revealed that on day zero after duct deligation, there were moderate atrophy in SMG lobes, loss of normal architecture and severe vacuolization within remaining ducts and acini. Under higher magnification we could distinguish prominent fibroblasts within CT fibers (Fig.1).

2. Masson trichrome:

At day zero after duct deligation, LM examination of tissue sections showed that there were thick CT capsule and septa. Plus, collagen fibers were coarse and surrounded the dilated blood vessels (Fig.2).

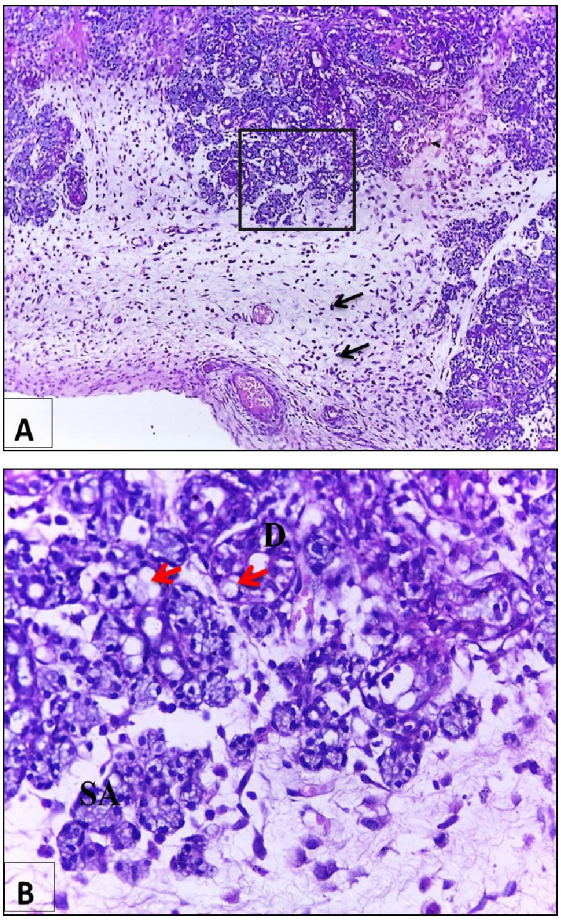

Fig. (1): Photomicrographs of right SMG of control group at day zero after duct deligation. **(A)** Lobes of SMG showing moderate atrophy and prominent fibroblasts (black arrows) within CT fibers. **(B)** Higher magnification of black boxed area at (A) showing loss of normal architecture with severe cytoplasmic

vac
and

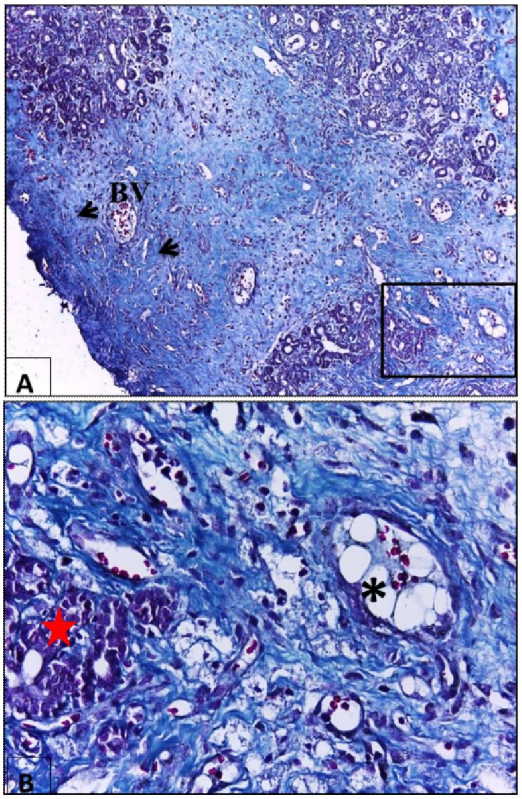

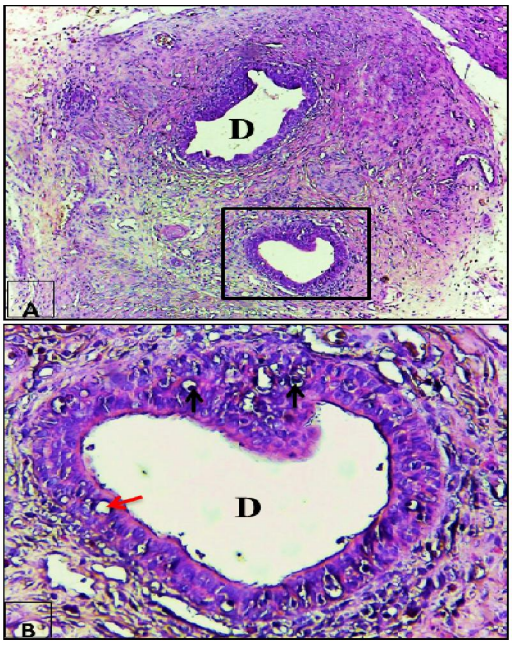

Fig
gro
lob
wit
col
ma
thic
and
tric

B)
1.

rev
sev
intr
ren
stra
son
vac

2.

of tissue sections showed that intralobar ducts were surrounded by increased amount of collagen fibers which appeared coarse with haphazard course. Also, very thick CT capsule with inflammatory cells infiltration were also seen (Fig.4).

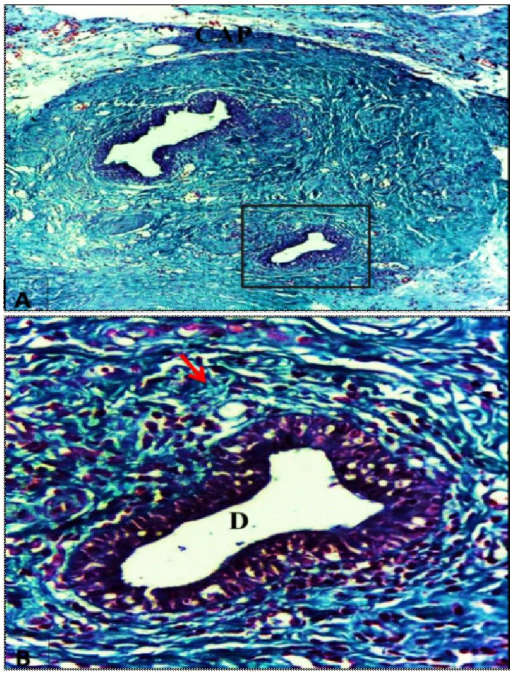

Fig. (4): Photomicrographs of right SMG of control group at day 3 after duct deligation. **(A)** Atrophied lobe of SMG showing an increase in collagen fiber. **(B)** Higher magnification of black boxed area at (A) showing an intralobar duct (D) surrounded by coarse collagen fibers run in haphazard course (red arrow). (Masson's Trichrome stain, A x 100 and B x 400).

C) Day seven:

1. **Haematoxylin and Eosin:**

The examination of SMG lobes showed loss of normal architecture with severs atrophy of acini and ducts. Also, the acinar cells had many coalesced cytoplasmic vacuolization (Fig.5).

2. **Masson trichrome:**

On the seventh day after duct deligation, CT capsule depicted coarse collagen fibers with haphazard orientation. Also, the degenerated acini either invaded or surrounded by thick fibrous CT (Fig.6).

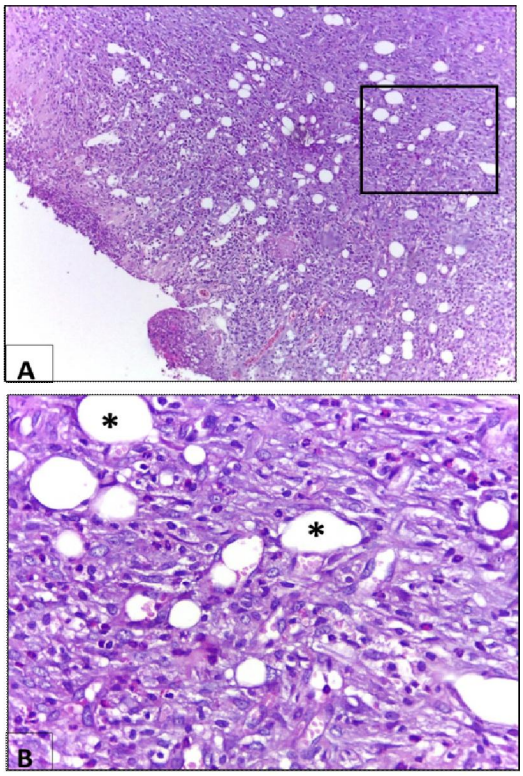

Fig. (5): Photomicrographs of right SMG of control group at day 7 after duct deligation **(A)** Lobes of SMG showing loss of normal architecture. **(B)** Higher magnification of black boxed area at (A) showing severs atrophy of acini and ducts. Also, acinar cells have many coalesced cytoplasmic vacuoles (*). (H & E stain, A x 100 and B x 400).

D) Day fourteen:

1. Haematoxylin and Eosin:

At day 14 after duct deligation, LM examination showed that SMG lobes had sever atrophy, and loss of normal architecture. The remaining ducts showed apoptotic cells on their lining with stagnation of salivary secretion in the duct lumen. Also, intralobar fatty degeneration could be illustrated (Fig.7 and 8).

2. Masson trichrome:

Light microscopic examination showed large blood vessels engorged with RBCs and they were surrounded with coarse collagen fibers which took haphazard course. Also, the degenerated acini and ducts were invaded by fibrous tissue with moderate inflammatory cells infiltrates (Fig.9).

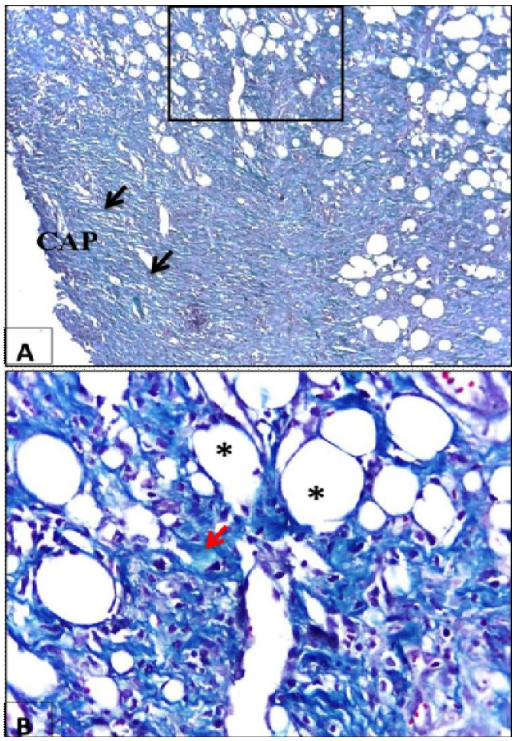

Fig. (6)

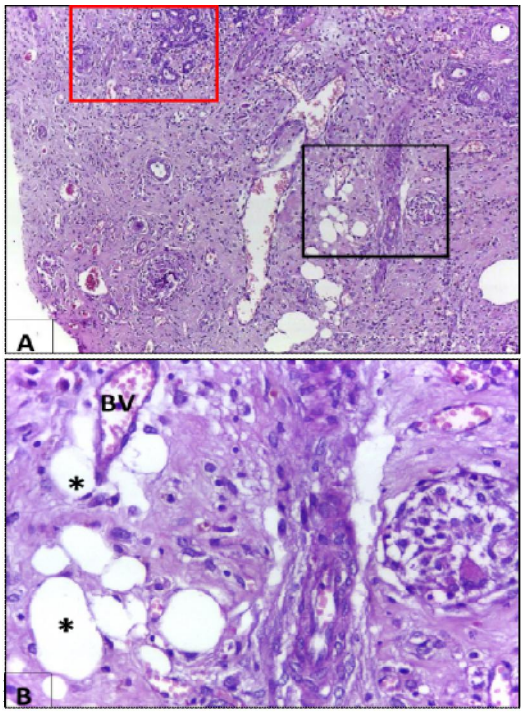

Fig. (7)

Fig. (6): Photomicrographs of right SMG of control group at day 7 after duct deligation. **(A)** Atrophied lobes of SMG, and CT capsule consists of coarse collagen fibers with haphazard orientation (black arrows). **(B)** Higher magnification of black boxed area at (A) showing thick fibrous CT (black arrow) invading and surrounding the degenerated acini (*). (Masson's Trichrome stain, A x 100 and B x 400). (Mic. Mag. X 1000).

Fig. (7): Photomicrographs of right SMG of control group at day 14 after duct deligation. **(A)** lobes of SMG showing sever atrophy. **(B)** Higher magnification of black boxed area at (A) showing intralobar fatty degeneration (*) and dilated blood vessel (BV) with extravasated RBCs. (H & E stain, A x 100 and B x 400).

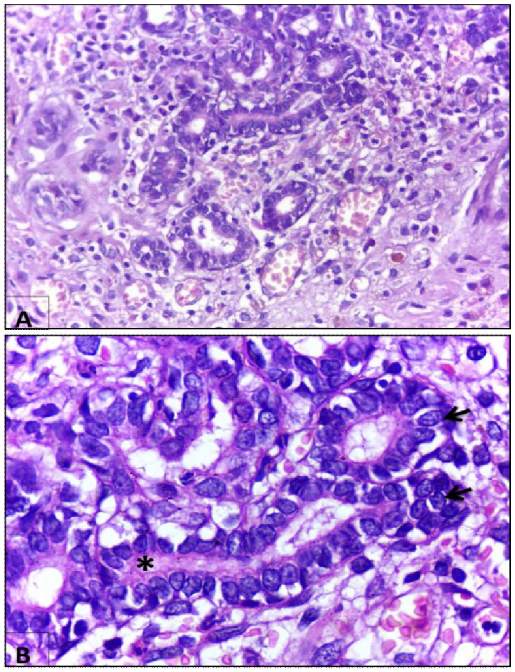

Fig. (8): (A) Higher magnification of red boxed area at the previous figure. **(B)** Apoptotic like cells on the duct lining (black arrows) with partial loss of the cell junction can be seen. Stagnation of salivary secretion in the duct lumen (*) can be detected. (H & E stain, A x 400 and B x 1000).

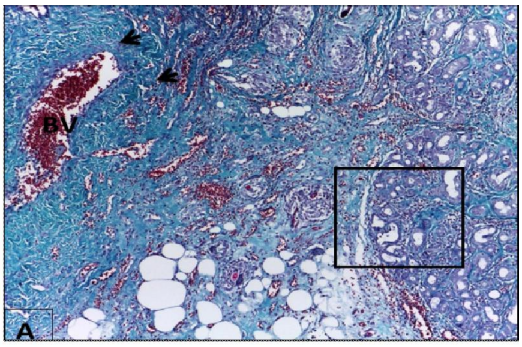

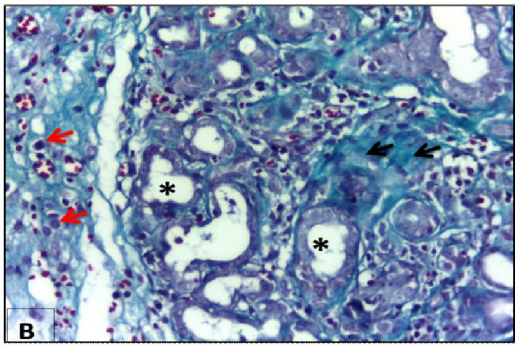

Fig. (9): Photomicrographs of right SMG of control group at day 14 after duct deligation. **(A)** Atrophied lobes of SMG and large blood vessel (BV) that is engorged with RBCs and surrounded with coarse collagen fibers which run in haphazard manner (black arrows). **(B)** Higher magnification of black boxed area at (A) showing the degenerated acini and ducts (*) are invaded by fibrous tissue (black arrows) with moderate inflammatory cells infiltration (red arrows). (Masson's Trichrome stain, A x 100 and B x 400).

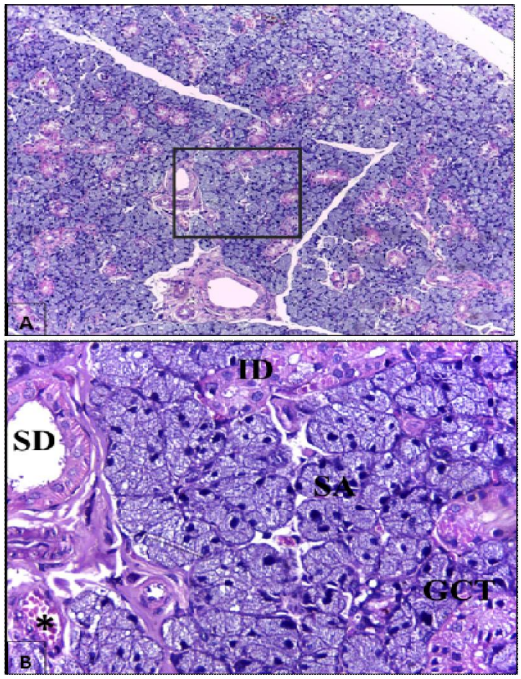

Fig. (10): Photomicrographs of left SMG of control group at day zero after duct deligation showing. **(A)** Lobes of SMG with almost normal architecture. **(B)** Higher magnification of black boxed area at (A) showing SA with pyramidal shaped cells and basally located nuclei, ID appears lined with simple cuboidal cells with centrally located nuclei, and SD appears lined with simple columnar epithelium with round nuclei and basal striations near normal small endothelial venules (*). Also, GCT appears lined with columnar cells with basally situated nuclei and apically eosinophilic granules. (H & E stain, A x 100 and B x 400).

(2) Negative control group (left side):-

We found that LM examinations of the tissue sections of the negative control SMGs showed nearly the same histological appearances.

A) Day zero:

- **Haematoxylin and Eosin:**

Light microscopic examinations left SMGs of control group at day zero after duct deligation illustrated that there were normally appeared seromucous acini with pyramidal shaped cells and basally located nuclei. In addition, ID appeared lined with simple cuboidal cells with centrally located nuclei. Also, SD appeared lined with simple columnar epithelium with basally located nuclei and basal pink striations and near normal small endothelial venules. Also, GCT appears lined with columnar cells with basally situated nuclei and apically eosinophilic granules (Fig.10).

- **Masson trichrome:**

Microscopic examination left SMGs of control group at day zero after duct deligation exemplified that lobes of SMG were surrounded with almost normal moderate size CT capsule which send thin CT septa containing fine collagen fibers. Also, collagen fibers in CT stroma around serous acini appeared thin with normal orientation (Fig.11).

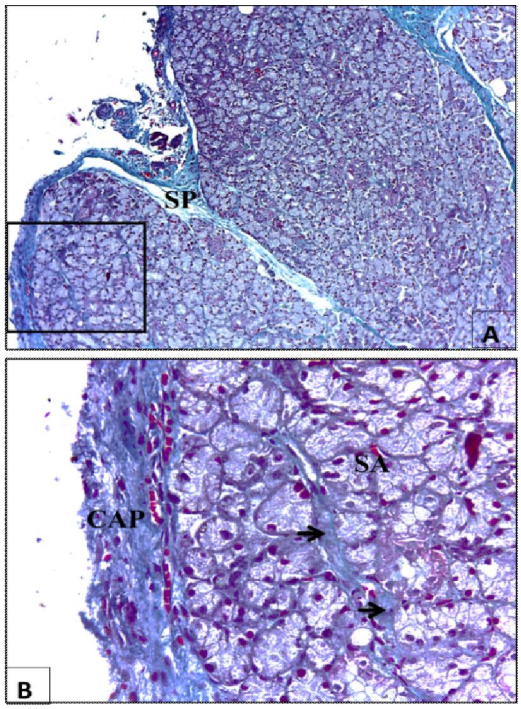

Fig. (11): Photomicrographs of left SMG of control group at day zero after duct deligation. **(A)** Lobes of SMG that are separated with thin CT septa (SP) which contain fine collagen fibers. **(B)** Higher magnification of black boxed area at (A) showing moderate size CT capsule (CAP) and thin collagen fibers (black arrow) in CT stroma around SA. (Masson's Trichrome stain, A x 100 and B x 400).

B) Day three, seven and fourteen:

The results of these periods were similar to the results of day zero of negative control group.

II. PRP group:-

1) positive group (right side):

A) Day zero:

The results of this follow up period were the same of its analogous of the positive control group.

B) Day 3:

1. **Haematoxylin and Eosin:**

Light microscopic examination of tissue sections for right SMG of PRP group at day 3 after duct deligation showed that, there were lobar atrophy and loss of normal acinar architecture (Fig.12).

2. Masson trichrome:

Thin CT capsule and thick CT septa were depicted in this period. Coarse collagen fibers showed around enlarged blood vessels that engorged with RBCs (Fig.13).

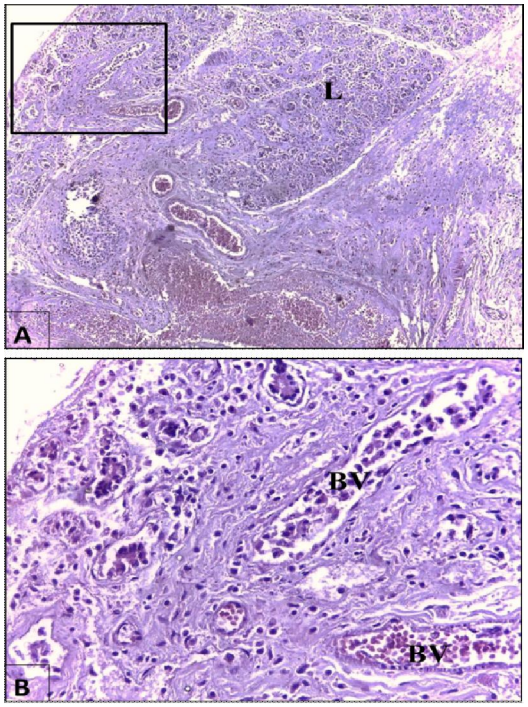

Fig. (12): Photomicrographs of right SMG of PRP group at day 3 after duct deligation **(A)** SMG with atrophic lobes (L). **(B)** Higher magnification of black boxed area at (A) showing loss of normal acinar architecture of SMG and dilated blood vessels (BV) that are engorged with RBCs. (H & E stain, A x 100 and B x 400).

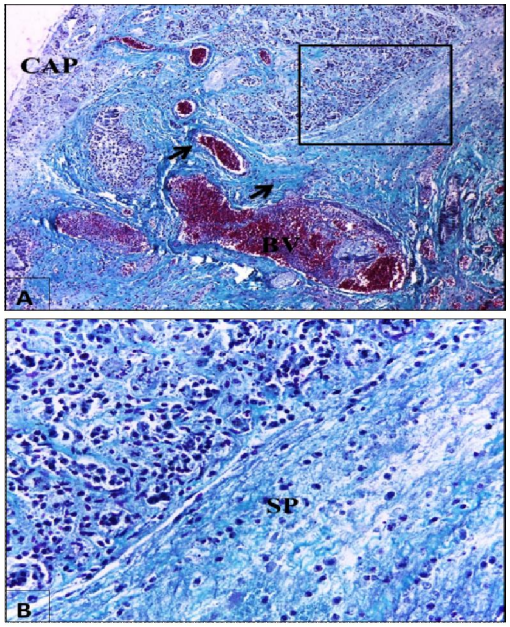

Fig. (13): Photomicrographs of right SMG of PRP group at day 3 after duct deligation showing **(A)** Lobes of SMG that are surrounded with thin CT capsule, and enlarged blood vessels (BV) that engorged with RBCs and surrounded by coarse collagen fibers (black arrows). **(B)** Higher magnification of black boxed area at (A) showing thick CT septa (SP). (Masson's Trichrome stain, A x 100 and B x 400).

C) Day 7:

1. **Haematoxylin and Eosin:**

Light microscopic examination of tissue sections for right SMG of PRP group at day 7 after duct deligation showed that, there were branched duct like tubules in-between serous acini, prominent vacuolization within the acini, and widening of inter acinar space (Fig.14). Also, multiple mitotic figures and binucleated acinar cells could be depicted (Fig.15).

2. **Masson trichrome:**

Normal structure of CT capsule and septa with extravasated RBCs could be detected. In addition, CT stroma with fine normal collagen fibers and high endothelial venule were detected in the parenchymal part of the gland (Fig.16).

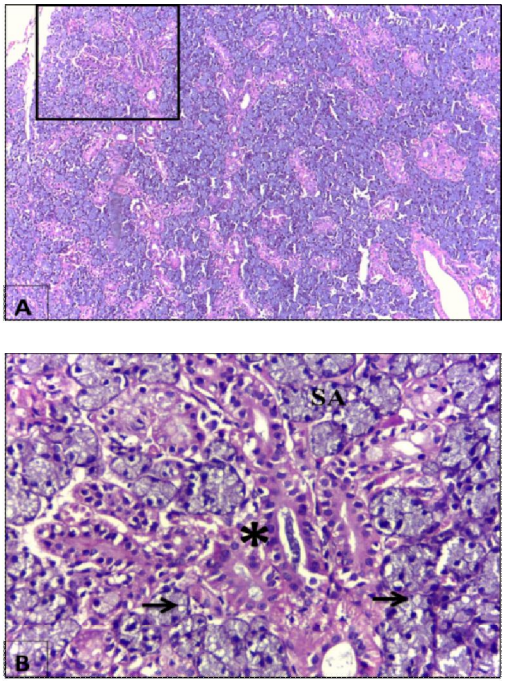

Fig. (14): Photomicrographs of right SMG of PRP group at day 7 after duct deligation **(A)** Lobe of SMG. **(B)** Higher magnification of black boxed area at (A) showing branched duct like tubules (*) in-between serous acini, prominent vacuolization within the acini (black arrows). (H & E stain, A x 100 and B x 400).

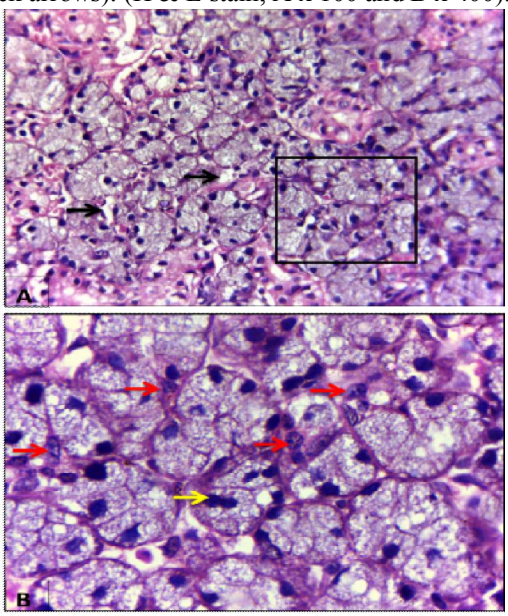

Fig. (15): Photomicrographs of right SMG of PRP group at day 7 after duct deligation **(A)** Lobe of SMG showing widening of inter-acinar space (black arrows). **(B)** Higher magnification of black boxed area at (A) showing multiple mitotic figures (red arrows) and binucleated acinar cells (yellow arrow). (H & E stain, A x 400 and B x 1000).

C) Day 14:

1. **Haematoxylin and Eosin:**

Light microscopic examination of tissue sections for right SMG of PRP group at day 14 after duct deligation showed lobes of SMG with almost normal architecture and recovery of serous acini with few cytoplasmic vacuolization. The branched duct like tubules ending with serous acini and almost normal SDs could be detected around large endothelial venules (Fig.17). Multiple mitotic figures and binucleated cells were clearly seen (Fig.18).

2. **Masson trichrome:**

Thick CT capsule with inflammatory cell infiltration was detected. Fine collagen fibers were clearly seen in CT stroma with increased vascularity (Fig.19).

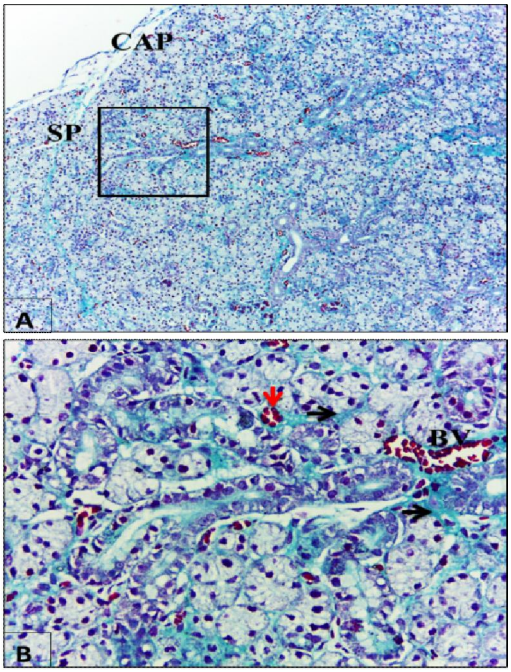

Fig. (16): Photomicrographs of right SMG of PRP group at day 7 after duct deligation. **(A)** Lobe of SMG showing CT capsule and septa with normal structure. **(B)** Higher magnification of red boxed area at (A) showing CT stroma with fine normal collagen fibers (black arrows) and high endothelial venule in the parenchymal part of the gland (red arrow). (Masson's Trichrome stain, A x 100 and B x 400).

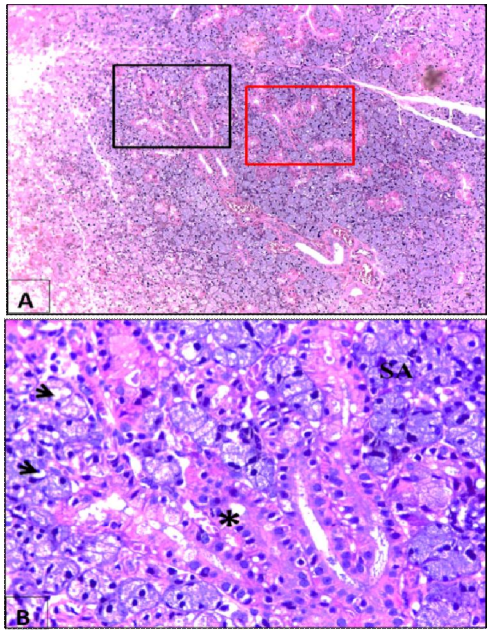

Fig. (17): Photomicrographs of right SMG of PRP group at day 14 after duct deligation **(A)** Lobes of SMG with almost normal architecture. **(B)** Higher magnification of black boxed area at (A) showing recovery of serous acini with some cytoplasmic vacuolization (black arrows) and branched duct like tubules (*) ending with serous acini. (H & E stain, A x 100 and B x 400).

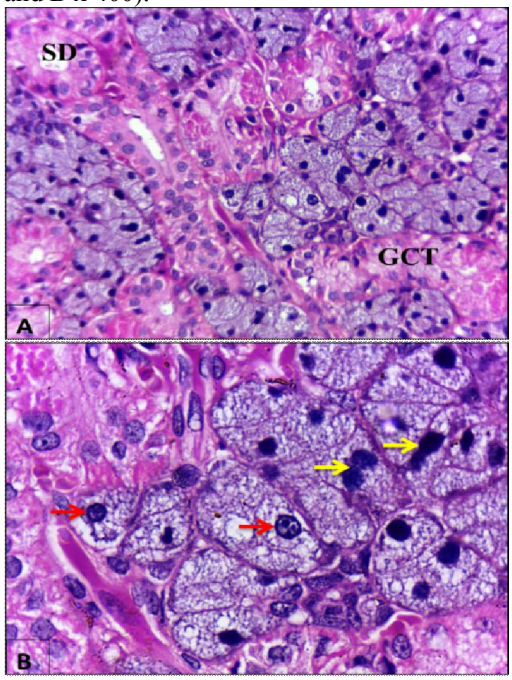

Fig. (18): (A) Higher magnification of red boxed area at the previous figure showing almost normal SDs and GCT. **(B)** Multiple mitotic figures (red arrows) and binucleated cells (yellow arrows) are clearly seen. (H & E stain, A x 400 and B x 1000).

2) Negative group (left side):-

The results of all follow up periods of Left SMGs of PRP group showed the same results for day zero of the negative control group.

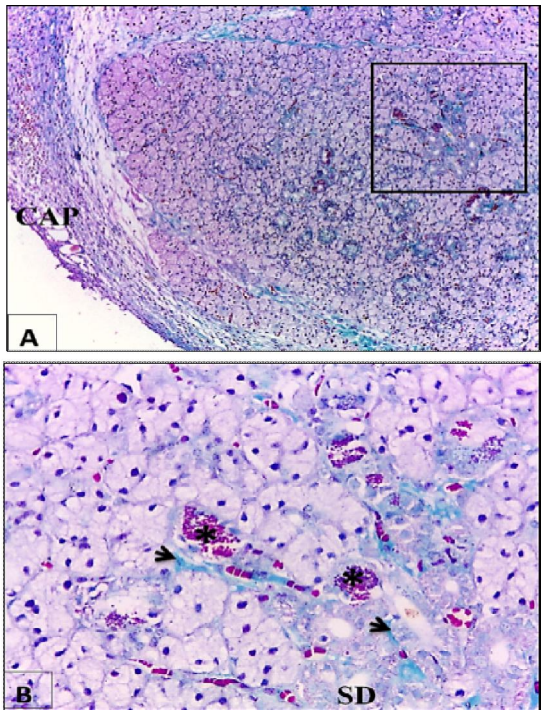

Fig. (19): Photomicrographs of right SMG of PRP group at day 14 after duct deligation showing. **(A)** Lobes of SMG with thick CT capsule (CAP). **(C)** Higher magnification of black boxed area at (A) showing CT stroma that has fine collagen fibers (black arrows) and increased vascularity (*). (Masson's Trichrome stain, A x 100 and B x 400).

4. Discussion

In this study we preferred the extra oral rout of SMD ligation of albino rat as a model of duct obstruction because it is a convenient and reproducible method (13). In this model the chorda tympani nerve could be included during the duct ligation as its terminal part is on the rat SMD [14,15]. Additionally, previous studies showed that there was irreversible atrophy of SMG when chorda tympani nerve was included in the duct ligature compared with exclusion of the nerve as the parasympathetic nerve has atrophic effect on SGs [5,16].

In this work, duct ligation was persisted for two weeks in order to allow progression of the severe SMG atrophy that was declared by Okazak et al. [17]. After that, evaluation of the regeneration was conducted in the experimental periods of 3, 7, and 14 days follow the protocol of Schwarz et al. [18], Cotroneo et al. [19], and Osailan et al. [20].

Until the present research, studies of the effect of PRP treatment on SGs were not be available, PRP was used in treatment in this study because it had given promising results in other tissues on regenerative therapy studies such as treatment of acute and chronic injuries, wound healing, regeneration of soft and hard tissues, healing of ulcers and burns, stimulation of osseous tissue regeneration in dentistry, implantology, maxillofacial and plastic surgery, knee osteoarthritis and repair of musculoskeletal tissue lesions in sports medicine [21]. Besides, PRP were evaluated recently in neural repair [22]. Interestingly, Human studies had also shown that PRP can be advantageously and easily applied in dental and cosmetic surgery [23]. Noteworthy, there are different protocols in PRP preparation and platelet activation. Almost all of PRP preparation protocols include centrifugation of the whole blood that separates the blood cells from the plasma and platelets [24].

As the centrifugation force is a critical step in PRP preparation, in the current study we followed the protocol of Dolder et al. [11] using single-step centrifugation of 800 RPM for 15 min, the least mechanical forces could separate the plasma to avoid platelets damage and the consequence of losing the granular load of the growth factors [25]. Also, there were reports suggesting that spins greater than 800 RPM might cause decrease in the amount of some growth factors [26]. We used sodium citrate because it was suggested as an anticoagulant with no negative effects on PRP preparation than other types of anticoagulants that were reported to be harmful to the platelets [27]. Moreover, the use of a centrifugation-based separation causes direct platelet activation without addition of activators and the PRP becomes ready to inject, thus we didn't use calcium chloride nor thrombin that transform PRP into insoluble gel [28] also we didn't use collagen type I as it stimulates a rapid release of growth factors that remains stable up to 24 h then degraded [29]. Local injection of the PRP into the macroscopic center of SMG was performed at the time of PRP preparation to avoid loss of growth factors over the time as they have short half-life (from minutes to hours) after their release from the platelets and they might be degraded before tissue receptors interactions [30]. In this study, we locally injected PRP (0.5 mL/kg body weight) [platelet count, 824 × 10^3/□L] into the center of SMG at the time of deligation following the suitable dose of Hesami et al. protocol [12].

In negative control group, qualitatively LM results of the unligated left SMGs showed almost normal histological appearances for all groups. These results were in accordance with that of previous studies which found that SMG morphology appeared normal in contralateral left side after intraoral SMD

ligation of right SMG for one day [31] and after extra oral SMD ligation for 7 days [32]. In contrary, Walker & Gobe [33] found that compensatory hyperplasia was occurred to the left parotid gland when the right one was ligated.

Noteworthy, LM results of ligated right SMGs of positive control group revealed marked degenerative changes persisted on all follow up periods. The severity of these changes was increased gradually from day zero to 14. This result was in agreement with several studies which declared that there was irreversible SMG atrophy following extra oral SMD ligation [5,16]. Also, Peronace et al. [34] confirmed that parasympathetic denervation of rat SMG cause severe irreversible atrophy after 16 days and they attributed this result to the trophic function of this nerve. In contrary, Cotroneo et al. [19] found that H & E histological examination of the 3, 5 and 7 days deligation, after intraoral SMD ligation for two weeks, showed that SMGs exhibited normal morphology.

At the light microscopic level using H & E stain, there was sever SMG atrophy included the parenchymal elements and only the intralobar ducts could be distinguished in all follow up periods. The same findings were confirmed by Silver et al. [35] who qualified these results to activation of the mammalian target of rapamycin (mTOR) pathway and overexpression of autophagy related proteins which might be led to autophagy activation after 3 days of SMG ligation and continued throughout the two weeks of ligation. Similarly, Scott et al. [36] found that in totally obstructed parotid glands a rapid, progressive severe atrophy amounting to absolute losses of over 85% of parenchymal tissue after two weeks and remaining intralobular epithelia consisted of extremely atrophic acini and numerous duct-like structures with intermediate forms. Also, they attributed these results to direct damage resulting from back-pressure of the execratory duct contents that was accompanied by inflammatory changes within the gland and further cytological damage and atrophy. Moreover, they suggested that the increased number of duct-like structures that greatly exceeds the number of profiles of ID and SD in the lobules of normal glands might be derived from surviving atrophic acini since the central acinar lumens became distended with fluid secretion. In addition, Johnson [37] accredited these atrophy to the changes described in disuse atrophy, where failure of secretion led to internal cellular dismantling of stored granules and consequent acinar and glandular shrinkage. Besides, at day 3 after duct deligation there was dilatation of the intralobar ducts. This was in agreement with the finding of Scott et al. [36] who attributed the dilatation of the intralobar ducts of parotid gland to the raised intraductal pressure due to collected secretion proximal to the ligature suture. On other hand, both acinar and ductal cells of SMG exhibited some areas of cytoplasmic vacuolization. This was in accordance with previous studies which found that cytoplasmic vacuoles were appeared in SMG tissue at the first three days after duct ligation and after 3 days from deligation [6,38]. Myers and Mcgavin [39] attributed cytoplasmic vacuolization in SGs as an early form of degeneration that manifested as increased cell size and volume resulting from an overload of fluid caused by a failure of the cell to maintain normal homeostasis. Nonetheless, Shaposhnikov [40] described the occurrence of cytoplasmic vacuoles as age-related ultra-structural features in the adrenal cortex of old rats. Also, Majno and Joris [6] reported that some cytoplasmic vacuoles were neutral fat droplets and might be feature on the pathway of cell death and necrosis. On the other hand, at day 3 after duct ligation the remaining intralobar ducts showed stratifications of their lining. El Tahawy et al. [41] found the same result on the intralobar ducts of pancreas after induction of diabetes. They suggested that it might be a trial to increase the cell numbers as a way for regeneration of β-cells.

Likewise, at the light microscopic level using Masson Trichrome stain, there were increased amount of collagen fibers deposition in both CT capsule and septa that could invade the degenerated acini and ducts at nearly all the time intervals. Furthermore, the collagen fibers were seemed coarse with haphazard course. These findings were in agreement with previous studies which found that there was rapid SMG fibrosis after two week from ligation [32,36]. Also, Zaia et al. [42] found that glandular atrophy was accompanied by a rapid increase in collagen deposition in capsular, septal and intralobular regions after mice SMG ligation for two weeks, and they attributed this result to up regulation of Transforming growth factor-β (TGF-β) and their receptors in the SMG following SMD ligation. Furthermore, Hashimoto et al. [43] interpreted the interrupted size and course of collagen fibers to marked reduction in the synthesis of several growth factors responsible for regulation of collagen deposition as S-100 protein and EGF that was shown to be reduced in SMD ligation of rats. On the other hand, inflammatory cell infiltrations around CT were appeared at follow up periods 3 and 14. These findings were in agreement with Scott et al. [36] who found that chronic inflammatory infiltrate in parotid gland was mainly intralobular and of variable intensity after ligation for two weeks. Also, Standish and Shafer [44] found that infiltrates of neutrophils were occurred in the early stage of SMD ligation followed by monocytes invasion. However, Woods et al. [45] suggested that after SMD ligation of mice there was an increase in P2X7R activation that responsible for neutrophil, monocyte, macrophage, and T-cell

infiltration on the ligated SMG and production of inflammation that likely contribute to SMG degeneration. Plus, Tamarin [46] found that leukocytes and eosinophil could be infiltrated to the ligated SMG at the later stages of ligation (two weeks) after neutrophils and monocytes which infiltrated at the earlier stages. He suggested that phagocytic action of these motile cells was important to compensate the obliteration of the normal secretion escape route so that secretion products and cell debris could be removed and the in situ action of autolytic enzymes was avoided. Interestingly, in the current study wide intercellular spaces were detected between some acinar and ductal cells of ligated SMG, which could indicate possible secretion and/or pathway through the basolateral plasma membrane.

The effect of PRP in our study could be explained in the light of many studies that associated the efficiency of PRP to the different growth factors and bioactive substances that entrapped within α-granules and orchestrated the tissue regeneration (48). Theses growth factors include platelet-derived growth factor (PDGF), transforming growth factors (TGF-β1 and TGF-β2), IGF-1, vascular endothelial growth factor (VEGF), interleukin-1 (IL-1), interleukin-6 (IL-6), interleukin-8 (IL-8), TNF-a, basic fibroblast growth factor (bFGF), keratinocyte growth factor (KGF), and connective tissue growth factor (CTGF) [25,49,50].

Noteworthy, cellular proliferation and regeneration are important functions of PRP. The binding of PDGF with its receptors induces cellular proliferation and migration [51,52]. Also, PDGF and TGF-β act synergistically to enhance ECM deposition and CT cell proliferation in wound healing. In the kidney, glomerular mesangial cells proliferate and secrete ECM in response to PDGF and TGF-β[53,54]. Importantly, IGF-I has profound effects on stimulating growth by increasing the proliferation of many cell types including fibroblasts. It functions best in conjunction with other growth factors such as PDGF [55]. Basic fibroblast growth factor has many biological activities that stimulate the proliferation of fibroblasts and capillary endothelial cells and promote angiogenesis. Therefore, bFGF was selected in anticipation of promoted tissue regeneration [56]. Also, Keratinocyte growth factor has been shown to stimulate epithelial cell differentiation and it appears to control the proliferative-differentiative program from basal to suprabasal cells in the skin. Moreover, KGF has been shown to stimulate proliferation and to exert an anti-apoptotic effect for epithelial cells, which are of major importance for the post-traumatic wound healing [57]. However, Connective tissue growth factor is a unique growth factor that stimulates the proliferation and differentiation. It was reported that, it is involved in embryonic development, tissue repair, and tumor suppression [58].

As well as, PRP stimulate angiogenesis through VEGF, bFGF, key regulators of angiogenesis, their activation help capillary endothelial cells regeneration and promote angiogenesis [50]. Mammoto et al. [59] reported that PRP extract promotes angiogenesis through the angiopoietin1-Tie2 pathway that stimulates endothelial cell growth, migration and differentiation in cultured human dermal microvascular endothelial cells in-vitro and neonatal mouse retinal angiogenesis in-vivo.

Furthermore, Anti-inflammatory function of PRP comes from IL-1, IL-2, IL-6, together with TNF-á. Interlukin-1 enhances the proliferation of T-helper cells and growth and differentiation of B cells. Also, IL-1 induces the release of IL-2 when it secreted in larger quantities which is a mediator of inflammation by entering the blood stream and inducing synthesis of acute phase proteins [60]. In addition, IL-6, together with TNF-á and IL-1 induce the acute phase response of infection and corticosteroid release as part of an attempt to maintain homeostasis [61]. Besides, IL-8 is a chemotactic for lymphocytes and neutrophils. it is also angiogenic factor that involved in the pathogenesis of chronic angiogenesis-dependent inflammation such as rheumatoid arthritis, tumor growth, and wound repair [62].

Recommendation:

From the present study it could be recommended that:

- Further clinical and histological studies with different parameters are needed to evaluate the effect of the long term treatment using PRP in SGs.
- Further studies with different parameters are needed to evaluate the effect of PRP in other dental tissues.

References

1. Nanci A. Ten cate's oral histology: development, structure, and function. 8th ed. Salivary Glands: Mosby: Elsevier Health Sciences; 2013. 253-77.
2. Kumar GS. Orban's oral histology & embryology. 13th ed. Salivary Glands: Elsevier Health Sciences; 2011. 292-312.
3. Daniels TE, Wu AJ. Xerostomia--clinical evaluation and treatment in general practice. J Calif Dent Assoc. 2000;28(12):933–41.
4. Grisius MM. Salivary gland dysfunction: a review of systemic therapies. Oral Surgery, Oral Med Oral Pathol Oral Radiol Endod. 2001;92(2):156–62.
5. Osailan SM, Proctor GB, McGurk M, Paterson KL. Intraoral duct ligation without inclusion of the parasympathetic nerve supply induces rat

submandibular gland atrophy. Int J Exp Pathol. 2006;87(1):41–8.
6. Hishida S, Ozaki N, Honda T, Shigetomi T, Ueda M. Atrophy of submandibular gland by the duct ligation and a blockade of SP receptor in rats. 2016;78:215–27.
7. Holmberg K V., Hoffman MP. Anatomy, biogenesis, and regeneration of salivary glands Kyle. Monogr Oral Sci. 2014;24: (301):1–13.
8. DeRossi RI, Carolina Anciliero de Oliveira Coelho AI, Silveira de Mello GI, Oliveira Frazílio III F, Rejane Brito Leal CI, Gonçalves Facco G V, et al. Effects of platelet-rich plasma gel on skin healing in surgical wound in horses. Acta Cirúrgica Bras. 2009;24(4):276–81.
9. Fu X, Fang L, Li X, Cheng B, Sheng Z. Enhanced wound-healing quality with bone marrow mesenchymal stem cells autografting after skin injury. Wound Repair Regen. 2006;14(3):325–35.
10. Okuda K, Kawase T, Momose M, Murata M, Saito Y, Suzuki H, et al. Platelet-Rich Plasma Contains High Levels of Platelet-Derived Growth Factor and Transforming Growth Factor-β and Modulates the Proliferation of Periodontally Related Cells In Vitro. J Periodontol. 2003;74(6):849–57.
11. Dolder J Van Den, Mooren R, Vloon APG, Stoelinga PJW, Jansen JA. Platelet-rich plasma: quantification of growth factor levels and the effect on growth and differentiation of rat bone marrow cells. Tissue Eng. 2006;12(11):3067–73.
12. Hesami Z, Jamshidzadeh A, Ayatollahi M, Geramizadeh B, Farshad O, Vahdati A. Effect of platelet-rich plasma on CCl4-induced chronic liver injury in male rats. Int J Hepatol. 2014;2014:1-7.
13. Takahashi S, Shinzato K, Nakamura S, Domon T, Yamamoto T, Wakita M. Cell death and cell proliferation in the regeneration of atrophied rat submandibular glands after duct ligation. 2004;23–9.
14. Davis RA, Anson BJ, Budinger JM, Kurth L. Surgical Anatomy of the Facial Nerve and Parotid Gland Based upon a Study of 350 Cervico-facial Halves. Plast Reconstr Surg. 1958;21(1):84.
15. Harrison JD, Fouad HMA, Garrett JR. Variation in the response to ductal obstruction of feline submandibular and sublingual salivary glands and the importance of the innervation. J oral Pathol Med. 2001;30(1):29–34.
16. Proctor GBg, Garrett JR, Carpenter GH, Ebersole LE. Salivary secretion of immunoglobulin A by submandibular glands in response to autonomimetic infusions in anaesthetised rats. J Neuroimmunol. 2003;136(1):17–24.
17. Okazak H, Hattori T, Hishida S, Shigetomi T, Ueda M. Acceleration of rat salivary gland tissue repair by basic fibroblast growth factor. Arch Oral Biol. 2000;45(10):911–9.
18. Schwarz S, Huss R, Schulz-Siegmund M, Vogel B, Brandau S, Lang S, et al. Bone marrow-derived mesenchymal stem cells migrate to healthy and damaged salivary glands following stem cell infusion. Int J Oral Sci. 2014;6(3):154.
19. Cotroneo E, Proctor GB, Carpenter GH. Regeneration of acinar cells following ligation of rat submandibular gland retraces the embryonic-perinatal pathway of cytodifferentiation. Differentiation. 2010;79(2):120–30.
20. Osailan SM, Proctor GB, Carpenter GH, Paterson KL, McGurk M. Recovery of rat submandibular salivary gland function following removal of obstruction: a sialometrical and sialochemical study. Int J Exp Pathol. 2006;87(6):411–23.
21. Burnouf T, Goubran HA, Chen TM, Ou KL, El-Ekiaby M, Radosevic M. Blood-derived biomaterials and platelet growth factors in regenerative medicine. Blood Rev. 2013;27(2):77–89.
22. Giorgetti M, Siciliano G. Platelet-rich plasma: the role in neural repair. Neural Regen Res. 2015;10(12):1920.
23. Man D. Harvey P, Brown W. The use of autologous platelet-rich plasma (platelet gel) and autologous platelet-poor plasma (fibrin glue) in cosmetic surgery. Plast Reconstr Surg. 2001; 107(1):229-37.
24. Ehrenfest D, Rasmusson L, Albrektsson T. Classification of platelet concentrates : from pure platelet-rich plasma (P-PRP) to leucocyte and platelet-rich fibrin. Trends in Biotechnology. 2009;27(3):158-67.
25. Nikolidakis D, Jansen JA. The biology of platelet-rich plasma and its application in oral surgery: literature review. Tissue Eng Part B Rev. 2008;14(3):249–58.
26. Dugrillon A, Eichler H, Kern S, Klüter H. Autologous concentrated platelet-rich plasma (cPRP) for local application in bone regeneration. Int J Oral Maxillofac Surg. 2002;31(6):615–9.
27. Anitua E. Plasma rich in growth factors: preliminary results of use in the preparation of future sites for implants. Int J Oral Maxillofac Implant. 1999;14(4):529–35.
28. Snyder EL, Calhoun BC. Topical platelet growth factor therapy: of lotions and potions. Transfusion. 2001;41(10):1186–9.
29. Cavallo C, Roffi A, Grigolo B, Mariani E,

Pratelli L, Merli G, et al. Platelet-Rich Plasma : The Choice of Activation Method Affects the Release of Bioactive Molecules. Biomed Res Int. 2016;2016:1–7.
30. Harrison S, Vavken P, Kevy S, Jacobson M, Zurakowski D, Murray MM. Platelet activation by collagen provides sustained release of anabolic cytokines. Am J Sports Med. 2011;39(4):729–34.
31. Correia PN, Carpenter GH, Osailan SM, Paterson KL, Proctor GB. Acute salivary gland hypofunction in the duct ligation model in the absence of inflammation. Oral Dis. 2008;14:520–8.
32. Woods LT, Camden JM, El-sayed FG, Khalafalla MG. Increased Expression of TGF- β Signaling Components in a Mouse Model of Fibrosis Induced by Submandibular Gland Duct Ligation. Plos One. 2015;1–24.
33. Walker NI, Gobé GC. Cell death and cell proliferation during atrophy of the rat parotid gland induced by duct obstruction. J Pathol. 1987;153(4):333–44.
34. Peronace AAV, Davison TA, Houssay AB, Perec CJ. Alterations in submandibular and retrolingual glands following parasympathetic denervation in rats. Anat Rec. 1964;150(1):25–33.
35. Silver N, Proctor GB, Arno M, Carpenter GH. Activation of mTOR coincides with autophagy during ligation-induced atrophy in the rat submandibular gland. Cell Death Dis. 2010;1(1):e14-10.
36. Scott J, Liu P, Smith PM. Morphological and functional characteristics of acinar atrophy and recovery in the duct-ligated parotid gland of the rat. J Dent Res. 1999;78(11):1711–9.
37. Johnson DA. Regulation of salivary glands and their secretions by masticatory, nutritional, and hormonal factors. salivary Syst. 1987;135–55.
38. Takahashi S, Nakamura S, Suzuki R, Islam N, Domon T, Yamamoto T, et al. Apoptosis and mitosis of parenchymal cells in the duct-ligated rat submandibular gland. 1998;32(6):457–63.
39. Myers RK, McGavin MD. Cellular and tissue responses to injury. Pathol basis Vet Dis. 2007;4:3–62.
40. Shaposhnikov VM. The ultrastructural features of secretory cells of some endocrine glands in aging. Mech Ageing Dev. 1985;30:123–42.
41. El Tahawy NF, Rifaai RA, Saber EA, Saied SR, Ibrahim RA. Effect of Platelet Rich Plasma (PRP) Injection on the Endocrine Pancreas of the Experimentally Induced Diabetes in Male Albino Rats: A Histological and Immunohistochemical Study. J Diabetes Metab. 2017;8(3).
42. Zaia AA, Coletta RD, Almeida OP, Line SRP. Expression of collagen and elastic fibers in duct - ligated submandibular glands of mice. Eur J Oral Sci. 1996;104(5 - 6):627–9.
43. Hashimoto J, Yamada K, Ogata K, Takai Y, Mori M. Immunoreaction of keratin, actin, S - 100 protein and rat - EGF in ductligated rat salivary glands. J oral Pathol Med. 1992;21(5):214–20.
44. Standish SM, Shafer WG. Serial histologic effects of rat submaxillary and sublingual salivary gland duct and blood vessel ligation. J Dent Res. 1957;36(6):866–79.
45. Woods LT, Camden JM, Batek JM, Petris MJ, Erb L, Weisman GA. P2X7 receptor activation induces inflammatory responses in salivary gland epithelium. Am J Physiol Physiol. 2012;303(7):C790–801.
46. Tamarin A. The leukocytic response in ligated rat submandibular glands. J Oral Pathol Med. 1979;8(5):293–304.
47. Wang J, Cawley NX, Voutetakis A, Rodriguez YM, Goldsmith CM, Nieman LK, et al. Partial redirection of transgenic human growth hormone secretion from rat salivary glands. Hum Gene Ther. 2005;16(5):571–83.
48. Nurden AT, Nurden P, Sanchez M, Andia I, Anitua E. Platelets and wound healing. Front Biosci a J virtual Libr. 2008;13:3532–48.
49. Eppley BL, Woodell JE, Higgins J. Platelet quantification and growth factor analysis from platelet-rich plasma: implications for wound healing. Plast Reconstr Surg. 2004;114(6):1502–8.
50. Kubota S, Kawata K, Yanagita T, Doi H, Kitoh T, Takigawa M. Abundant retention and release of connective tissue growth factor (CTGF/CCN2) by platelets. J Biochem. 2004;136(3):279–82.
51. Claesson-Welsh L. Platelet-derived growth factor receptor signals. J Biol Chem Ed. 1994;269(51):32023–6.
52. Kelly JD, Haldeman BA, Grant FJ, Murray MJ, Seifert RA, Bowen-Pope DF, et al. Platelet-derived growth factor (PDGF) stimulates PDGF receptor subunit dimerization and intersubunit trans-phosphorylation. J Biol Chem. 1991;266(14):8987–92.
53. Phan SH. Role of the myofibroblast in pulmonary fibrosis. Kidney Int Suppl. 1996;54:S46-8.
54. Poncelet A-C, De Caestecker MP, Schnaper HW. The transforming growth factor-βbgr/SMAD signaling pathway is present and functional in human mesangial cells. Kidney Int. 1999;56(4):1354–65.

55. Greenhalgh DG. The role of growth factors in wound healing. J Trauma Acute Care Surg. 1996;41(1):159–67.
56. Kawai K, Suzuki S, Tabata Y, Ikada Y. Accelerated tissue regeneration through incorporation of basic fibroblast growth factor-impregnated gelatin microspheres into arti " cial dermis. 2000;21:489–99.
57. Jeschke MG, Richter G, Höfstädter F, Herndon DN, Perez-Polo JR, Jauch KW. Non-viral liposomal keratinocyte growth factor (KGF) cDNA gene transfer improves dermal and epidermal regeneration through stimulation of epithelial and mesenchymal factors. Gene Ther. 2002;9(16):1065–74.
58. Nishida T, Kubota S, Kojima S, Kuboki T, Nakao K, Kushibiki T, et al. Regeneration of defects in articular cartilage in rat knee joints by CCN2 (connective tissue growth factor). J Bone Miner Res. 2004;19(8):1308–19.
59. Mammoto T, Jiang A, Jiang E, Mammoto A. Platelet rich plasma extract promotes angiogenesis through the angiopoietin1-Tie2 pathway. Microvasc Res. 2013;89:15–24.
60. Schett G, Dayer J-M, Manger B. Interleukin-1 function and role in rheumatic disease. Nat Rev Rheumatol. 2016;12(1):14–24.
61. Streetz K, Luedde T, Manns M, Trautwein C. Interleukin 6 and liver regeneration. Gut. 2000;47(2):309–12.
62. Koch A, Polverini P, Kunkel S, Harlow L, Luisa A, Elner V, et al. Interleukin-8 as a Macrophage-Derived Mediator of Angiogenesis. Science. 2016;258(5089):1798–801.

12/6/2018